3-8-2012

Eye-safe, 243-mJ, Rapidly Tuned by Injection-Seeding, Near-Infrared, Optical, Parametric, Oscillator-based Differential-absorption Light Detection and Ranging Transmitter

Robert J. Foltynowicz

Michael D. Wojcik

Journal of
Applied Remote Sensing

Eye-safe, 243-mJ, rapidly tuned by injection-seeding, near-infrared, optical, parametric, oscillator-based differential-absorption light detection and ranging transmitter

Robert J. Foltynowicz
Michael D. Wojcik

Eye-safe, 243-mJ, rapidly tuned by injection-seeding, near-infrared, optical, parametric, oscillator-based differential-absorption light detection and ranging transmitter

Robert J. Foltynowicz and Michael D. Wojcik
Space Dynamics Laboratory, 1695 North Research Park Way, North Logan, Utah 84341
robert.foltynowicz@usurf.usu.edu

Abstract. Here, we demonstrate and characterize a high-energy, eye-safe, spectrally narrow, and frequency-agile near-IR optical parametric oscillator (OPO). The injection-seeded, noncritical phase-matched (NCPM) potassium titanyle arsenate (KTA) and ring-cavity OPO was pumped in single longitudinal mode (SLM) at 7 ns full width at half maximum FWHM and 30 Hz, neodymium-doped yttrium aluminum garnet (Nd:YAG), generating 243 mJ per pulse OPO signal output with a conversion efficiency of 27%, spectral linewidth of 157 MHz, and approximately M^2 of 29. Also, we demonstrate a nonmechanical method to switch the frequency of the OPO at a rate of 2 Hz from 1535.036 to 1535.195 nm, which represents the on/off resonances of carbon dioxide, respectively. However, the switching rate can be extended into the MHz range and is limited by the electronics driving the diode laser. Given the performance results of our frequency-agile OPO, this transmitter has great potential as a source in DIAL applications.
 [DOI: 10.1117/1.JRS.6.063510]

Keywords: optical parametric oscillator; frequency-agile; injection-seeded; KTA; ring-cavity; eye-safe; differential-absorption light detection and ranging.

Paper 11116 received Jun. 30, 2011; revised manuscript received Oct. 26, 2011; accepted for publication Jan. 5, 2012; published online Mar. 8, 2012.

1 Introduction

The use of differential-absorption light detection and ranging (DIAL) techniques has been established as one of the most sensitive ways to measure atmospheric pollutants over long ranges.[1–3] However, to make these measurements over long ranges with parts-per-billion (ppb) sensitivities requires stringent requirements be imposed on the laser source. The laser source must have the following characteristics: high energy, short pulsewidth, narrow linewidth, tunable, and frequency agile.[4] High energy is required for long-range detection, short pulsewidths are required for range resolution, narrow linewidths are required for accurately measuring the absorption features, tunability is required for accessing spectral lines of interest, and frequency agility is needed to rapidly measure return signals of both on/off resonances. In addition, rapid frequency switching must occur on time scales less than 1 to 3 ms because beyond this time the atmosphere is not considered frozen and the volume of the atmosphere being measured will have changed.[5] The scope of this paper specifically looks at expanding the available methodologies to rapidly tune NIR sources for DIAL applications.

Historically, the most common transmitters used for DIAL measurements were dye lasers, solid-state lasers, line-tunable CO_2 lasers, and optical parametric oscillators (OPO). But in the infrared (IR), OPO sources have dominated.[4] The methods that were used to rapidly tune OPO sources generally relied on dual-wavelength injection-seeding of the cavity using diode lasers and a mechanical switching method (such as a crystal stepper motor or an acoustic-optic deflector) that was synchronized with alternating pulses of the pump laser to either rotate the OPO crystal or pump the beam angle.[6,7] An alternative frequency-agile method was used by Weibring et al that did not utilize injection-seeding of the OPO; instead they used

0091-3286/2012/$25.00 © 2012 SPIE

piezoelectric transducers to mechanically move a wavelength tuning mirror and the crystal angle tuning element.[8]

Therefore, the state-of-the-art techniques that rapidly tune near- to mid-infrared OPO sources are based on mechanical switching methodologies. In this paper, we describe the development of a nonmechanical method to rapidly switch wavelengths in near-infrared within a narrow spectral bandwidth. Recently, we demonstrated a 215 mJ per pulse, eye-safe (1.5 μm), OPO-based elastic lidar transmitter that is pumped by a single longitudinal mode (SLM), Nd: YAG at 1064 nm.[9] By making some minor modifications to our design and injection-seeding the OPO, here we demonstrate and characterize a nonmechanical, frequency-agile, NIR source that switches at 2 Hz (limited by the wavemeter's refresh rate) between actual on/off resonances of CO_2. The OPO produces 243 mJ per pulse of signal output with a 157-MHz linewidth, a tuning range between 1534.95 and 1535.45 nm, and an approximated M^2 of 29.

2 OPO Design

The OPO was pumped using a Continuum Powerlite 9030 Nd: YAG at 1064.162 nm$\pm$ 0.005 nm. The laser operated in SLM with a pulse repetition rate (PRF) of 30 Hz, and the YAG rod consisted of a flashlamp-pumped and Q-switched to produce 1 J per pulse output with a 7-ns full width at half maximum (FWHM) pulsewidth. Figure 1 shows the OPO cavity we used as well as the beam path for the pump, signal, and idler waves. Following the pump beam through the OPO cavity, the 1064-nm vertically polarized pump beam propagates through the output coupler (OC), which has a high transmission rate for the 1064-nm pump wave and 30% reflectivity for the 1535-nm signal wave. Once in the cavity, the pump beam passed through a $10 \times 10 \times 20$ mm^3, noncritical phase-matched (NCPM), KTA1 crystal that was X-cut at $\theta = 90$ deg and $\varphi = 0$ deg, where θ is the crystal cut angle in the xz plane. In the crystal, the pump generated an idler wave at 3468.300 nm and amplified a signal wave at 1535.200 nm. The polarization of the pump, signal, and idler waves were *o*, *o*, and *e*, respectively. All three beams entered a 1-in., right-angled, BK7, total internal reflection (TIR) prism, which was AR-coated for both 1064 and 1535 nm wavelengths. However, only the pump and signal waves were retroreflected towards KTA2. Upon exiting KTA2, the pump beam and the horizontally polarized idler beam passed through the high reflector (HR), but the signal wave reflected towards the OC. The HR was highly transmissive to the pump and idler and 99.5% reflective of the signal wave. The signal then exited from the OC and 30% of the signal wave power was fed back into the cavity, which established a singly resonant oscillator (SRO).

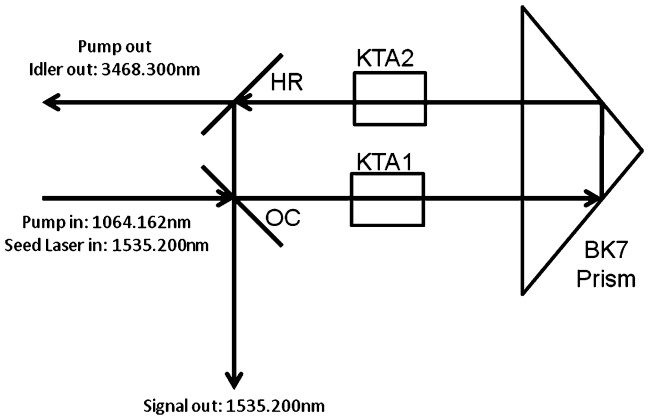

Fig. 1 Components and beam path diagram of the KTA, ring-cavity OPO. HR: high reflector (99.5%, 1535 nm, highly transmissive to 1064 and 3468 nm). OC: output coupler (highly transmissive to 1064 nm and 30% reflective of 1535 nm). KTA1 and KTA2 are NCPM, x-cut, $\Theta = 90$ deg, $\varphi = 0$ deg crystals with dimensions of $10 \times 10 \times 20$ mm^3.

3 OPO Injection Seeding

The major technical challenge to successfully injection-seed a TIR prism-OPO was addressing the scrambling of the phase relationships between the pump, signal, and idler waves as they propagated through the TIR prism to KTA2. When this phase relationship was modified at the exit of the TIR prism, the ability to seed this cavity significantly decreased. Therefore, in order to overcome this issue, we established an SRO cavity. Using this configuration, we eliminated the idler wave from the cavity and the phase relationship of the three waves did not need to be conserved. To configure the OPO to SRO, we had to use a TIR prism made with a BK7 substrate that had approximately 5% transmission at 3.5 μm for a 10-mm thick substrate.[10] In addition, we had to orient the polarization of the pump and the KTA crystals to generate a *p*-polarized idler wave. As a result, the idler generated from the KTA1 was absorbed by the BK7, and the TIR prism and the p-polarized idler generated from the second KTA was transmitted through the HR, leaving the signal wave to feed back into the cavity. To prevent temperature instabilities in the cavity due to both optical heating and environmental coupling, we placed an enclosure around the cavity with exit and entry windows while actively cooling the optical bench of the OPO with a TEC at 15°C. In addition, for precise wavelength control, one needs to incorporate the Pound-Drever-Hall cavity-locking method with a piezo-transducer mounted on the HR of the OPO.

The procedure we used to injection-seed the ring cavity of the OPO included matching the seed laser and pump polarizations, aligning the OPO cavity to optimize the transmission of the longitudinal cavity modes, spatially overlapping the seed and the pump beam at the OC of the OPO, and frequency-matching the seed beam with the longitudinal mode of the OPO cavity.

The seed laser used was a 14-pin butterfly, pig-tailed package, Anritsu, SLM, distributed feedback (DFB), diode laser with a center wavelength of 1535.200 nm. It had a 3-nm tuning range and produced 20 mW of output power with a spectral linewidth of 10 MHz. The DFB also had a polarization-maintaining fiber that vertically oriented the polarization of the light to match the pump polarization. In addition, we used collimation optics with the DFB to generate a 1.5-mrad, fully divergent, spherical beam.

OPO cavity alignment was accomplished by optimizing the transmission of the longitudinal cavity modes generated by the DFB seed laser that propagated through the OC while the pump beam was off. The cavity fringes were generated by current tuning the seed laser with a 10-Hz sawtooth waveform from a function generator coupled to the diode ILX driver (ILX Lightwave, Bozeman, MT). The transmitted cavity modes were detected using an E.O.T. 3000 InGaAs photodetector positioned after the HR, and the modes were displayed on an oscilloscope.

Once the OPO cavity was aligned, the seed beam was spatially expanded to match the diameter of the pump beam at the OC where both beams would copropagate into the OPO cavity. The seed beam was expanded by building a Galilean telescope with a $f = -9$-mm negative lens and a $f = +60$-mm positive lens to obtain an approximately 7× expansion.

Lastly, we frequency-matched the seed laser with the OPO cavity mode by upconverting the OPO signal frequency to 767.6 nm and using a 100-GHz free spectral range (FSR) etalon. Frequency-matching occurred by current tuning the DFB seed laser until the signal output of the OPO caused the wide etalon fringes to contract. More details on the purpose of upconverting the wavelength of the signal output of the OPO to its second harmonic is described in the next section.

3.1 *Monitoring the Seeding of the OPO*

To monitor whether the OPO was seeded or not, we not only observed the etalon fringes of the OPO output but also measured the reduction of the laser build-up time (RBUT) of the signal wave. Due to our limited beam diagnostic equipment to measure the tuning range of the unseeded OPO, we used a Coherent Wavemaster wavelength meter that had a detection range of 380 to 1095 nm. To access the operating range of our wavelength meter, we had to double the signal wave from 1535.200 nm to 767.600 nm. Since the apparatus was already setup with a 767.600 nm output, we decided to also monitor the seeding of the OPO at this wavelength using an etalon centered at 767.6 nm. Figure 2 shows the setup. The output of the OPO contained wavelengths of 1535.200 nm, 1064 nm, and 532 nm, which were the signal, pump, and second harmonic of the pump beam, respectively. The 1064 nm and 532 nm were

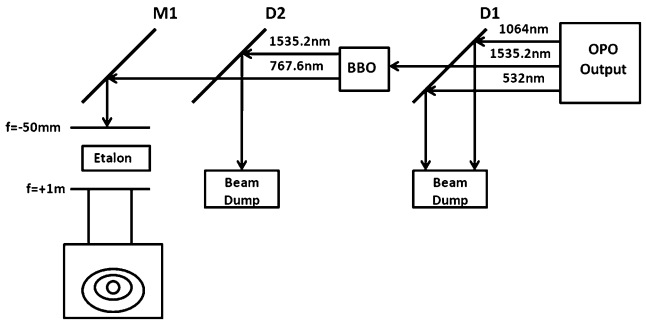

Fig. 2 Etalon fringe-monitoring setup. D1 and D2 are dichroic mirrors and M1 is a 767-nm turning mirror. The BBO is phase-matched to 20 deg and is 5-mm thick. The etalon has an FSR of 100 GHz and a mode FWHM of 6.3 GHz centered at 767 nm.

reflected away from the 1535.200 nm beam of interest using a dichroic mirror (D1). The transmitted 1535.200-nm beam propagated through a 20-deg cut BBO crystal ($10 \times 10 \times 5$ mm^3), which used Type I phase-matching to generate the second harmonic (SH) and 767.600 nm at a 20-deg phase-matching angle. The fundamental was filtered from the SH light using the dichroic mirror (D2), enabling the 767.600-nm light to reflect off the mirror (M1) and propagate through a monitoring etalon. The etalon system we designed to expand the SHG light using a -50-mm BK7 planoconcave diverging lens. The expanded beam then propagated through a 1-mm thick UV fused silica etalon with a FSR of 100 GHz, 6.3 GHz FWHM frequency mode width and a finesse of 16. The transmitted light from the etalon was focused using a 1-m focal length positive lens. The etalon fringes were monitored using an IR viewer by viewing a screen 1 m from the positive lens. The strongest injection-seeding occurred at a DFB wavelength of 1535.200 nm by pumping the OPO 2.5 times above threshold, which was 633 mJ. In addition to the etalon fringe monitoring, we confirmed the injection-seeding of the OPO by measuring the RBUT of the signal beam. We measured an RBUT of 1.2 ns, which equates to a reduction of about two roundtrips of the signal wave in the cavity.

4 Frequency Agility

The rapid tuning of our OPO was accomplished using a nonmechanical method. We exploited the idea of rapidly injection-seeding different modes into the OPO by using the current tunability of one DFB seed laser. At each alternate pulse of the pump laser, we current tuned the DFB seed laser to seed a new mode that was supported by the KTA bandwidth at the NCPM angle. The gain bandwidth at NCPM was narrow and, therefore, allowed frequency-tuning over a small range that was approximately 0.5-nm wide.

The nonmechanical method used to rapidly tune the OPO was accomplished by electrically tuning the seed laser via a square wave with voltages related to the target wavelengths and a frequency that was half the PRF of the pump laser using a Tektronix function generator. This waveform was triggered by the pump laser and coupled into the frontend of the ILX DFB driver that current tuned the seed laser to the desired wavelength.

To demonstrate our frequency-switching method, we simulated 20-GHz switching between the on/off resonances of a 13 GHz FWHM, CO_2 line centered at 1535.05 nm.[11] Due to the limitations of the refresh rate of our wavemeter, which was 4 Hz, we were only able to demonstrate the frequency agility of our OPO at a PRF of 2 Hz. However, a telecommunications DFB can be modulated to the GHz range, and the switching rate is limited by the frequency capability of the supporting electronics, such as the diode driver and function generator, to MHz ranges. Figure 3 shows the results of an 8-s section of a 1-min trial of our frequency-agility experiment. The OPO switched between the off-resonance (1535.194 nm) and the on-resonance (1535.036 nm) of CO_2 at a rate of 2 Hz. The DFB seed laser was tuned using a 1-Hz square wave with a 50% duty cycle and a voltage swing equivalent to a 20-GHz wavelength separation. Our data successfully shows that we can access and rapidly switch between frequencies for a CO_2 transition within the OPO's signal output bandwidth.

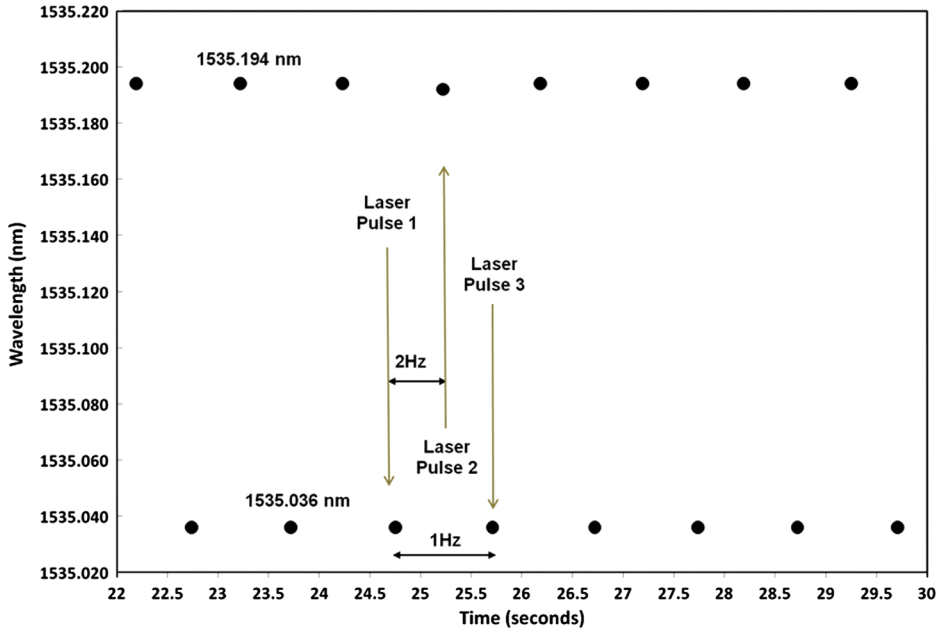

Fig. 3 This plot shows an 8-s section of the rapid tuning of the OPO at a rate of 2 Hz. The wavelengths were switched from 1535.036 to 1535.194 nm to emulate on/off resonances, respectively, of a CO_2 line spaced at 20 GHz. The wavelength switching was achieved by coupling a 1-Hz square wave into the current driver of the DFB seed laser at alternating pulses of the pump laser.

5 OPO Performance

The performance parameters we measured for the seeded KTA OPO were the pump oscillation threshold, maximum signal energy output, pump-to-signal conversion efficiency, full-angle divergence, KTA gain bandwidth (tuning range), and spectral linewidth.

Figure 4 shows a plot that compares the pump-to-signal energy conversion between the unseeded and the seeded OPO. In Fig. 4 it can be seen that injection-seeding the OPO resulted in a lower oscillation threshold (7.6 W, 51.4 MW/cm^2, 253 mJ) when compared to the unseeded OPO (8.3 W, 56 MW/cm^2, 277 mJ). The lowering of the oscillation threshold for the seeded OPO was expected due to the reduction of the signal beam but was facilitated by the seed laser. The seed laser enables the signal wave to exceed cavity losses and turn on quicker at lower pump intensities due to the elimination of the other modes that can be generated in the cavity. In addition, the general trend of the signal energy generated with the seeded OPO is systematically larger than the unseeded OPO for each pump energy level measured. The maximum signal energy produced by the seeded OPO was 243 mJ per pulse compared to the unseeded OPO of 138 mJ. In addition, the maximum conversion efficiency obtained for the unseeded and seeded OPOs were 16% and 27%, respectively. This 11% increase in the conversion efficiency of the seeded OPO has to do with the efficient conversion associated with an OPO that turns on earlier in the presence of a seed laser. In addition, injection-seeding lowers the pump intensity required to amplify the signal beam and, hence, reduces the back conversion which further facilitates better conversion efficiency.

The full-angle divergence for the OPO was measured using the technique of two distant points together with the knife-edge method to measure the respective beam diameters. The full-angle divergence measured was 6 mrad and the beam diameter at the signal output of the OPO was 9.34 mm. If we assume that the measured beam diameter at the OPO output is the beam waist, we can then calculate an estimate for the beam quality factor, M^2, using the following equation:

$$M^2 = \frac{\pi D \Theta}{4\lambda}, \tag{1}$$

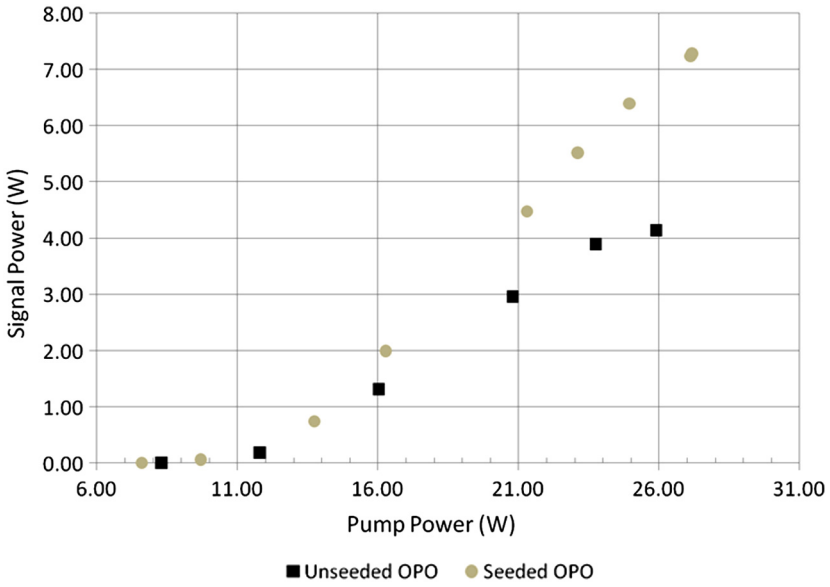

Fig. 4 Comparison between the unseeded and the seeded OPO pump-to-signal energy conversions. The gray circles represent the seeded OPO and the black squares represent the unseeded OPO. The pump source is a single mode, 30-Hz, Nd: YAG at 1064 nm. The maximum signal energies of the seeded and unseeded OPO were 243 mJ and 138 mJ, respectively.

where D is the measured beam diameter at the beam waist (mm), Θ is the measured full-angle divergence of the beam (mrad), and λ is the wavelength of the signal output of the OPO (1.5352 μm). The calculated M^2 is 29. If we expand this beam using a $5\times$ beam expander, which is normally done for Lidar OPO sources, the full-angle divergence is reduced to 1 mrad. This equates to an M^2 value of 4.8, which is quite suitable for matching the divergence between the transmitter and the telescope of a DIAL system.

The tuning range of the OPO is based on the gain bandwidth that is supported by the unseeded signal output at the NCPM angle. Due to the limited accessibility of the beam diagnostic equipment available in our lab, we had to indirectly approximate the tuning range by tuning a narrow linewidth (10 MHz) DFB seed laser to frequency-match each available longitudinal mode in the OPO. We continued tuning the DFB until we were unable to seed the OPO. The low and high wavelengths at which we were unable to seed the OPO were a proxy for the tuning band edges. Hence, we measured the power and the SH wavelengths at eight points in order to define the band center and the two edges of the tuning range. In essence, what we did was measure the seeding range of the signal wave at the NCPM angle of the crystal. The SH wavelengths were measured because of the operational range of our wavemeter, as described in Sec. 3.1. The measured results for the signal output tuning range was 47 GHz (1.6 cm^{-1}, 0.37 nm) at FWHM with a gain center at 1535.200 nm.

Again, due to our diagnostic equipment limitations, in order to obtain the spectral linewidth of the seeded signal output of the OPO, we measured its pulsewidth as opposed to using a scanning etalon. The etalon we used to monitor the OPO seeding was not appropriate for this measurement because its resolution was too low (100 GHz FSR). What was necessary was a scanning etalon with a FSR <150 MHz. Therefore, our best alternative was to measure the pulsewidth in time with the 1.5-μm signal output of the OPO. We used E.O.T.'s fast InGaAs photodetector with a response time <174 picoseconds. The resulting pulsewidth of the signal output was 2.8 ns. Assuming gaussian-shaped pulses, the time-bandwidth product was approximately equal to 0.44. Therefore, the spectral linewidth of our injection-seeded OPO was approximately 157 MHz.

6 Conclusions

In this investigation, we demonstrated and characterized an OPO source that is eye-safe, high-energy, and spectrally narrow. In addition, we developed a novel, nonmechanical method to

rapidly switch frequencies in the OPO by generating a square waveform that current tuned a single DFB seed laser. We demonstrated a frequency-switching rate of 2 Hz over a 0.5-nm tuning range with wavelengths separated by 20 GHz. In addition, the switching rate has the potential to be in the MHz range that is mainly limited by the electronics driving the seed laser.

The injection-seeded, KTA OPO produced a maximum of 243 mJ per pulse at 1535.2 nm with a conversion efficiency of 27%, a spectral linewidth of 157 MHz, and an M^2 of approximately 29. The overall performance and the rapid tuning capability of our OPO suggest that this source is a potential candidate for DIAL measurements.

To further develop our OPO-DIAL source, we intend to address the increasing interest of making atmospheric methane measurements. Our goal is to build a methane OPO at 1.6 microns and demonstrate its capability and rapid tuning using lab-based measurement that utilize an optical absorption cell filled with methane gas.

Acknowledgments

We would like to thank Arlee Smith for his efforts in modeling the performance of our OPO and his insightful discussions regarding seeding OPOs. This research was funded by Dugway Proving Grounds.

References

1. H. Kildal and R. L. Byer, "Comparison of laser methods for the remote detection of atmospheric pollutants," *Proc. IEEE* **59**(12), 1644–1663 (1971), http://dx.doi.org/10.1109/PROC.1971.8522.
2. R. M. Measures and G. Pilon, "A study of tunable laser techniques for remote mapping of specific gaseous constituents of the atmosphere," *Opt. Quant. Electron.* **4**(2), 141–153 (1972), http://dx.doi.org/10.1007/BF01421178.
3. R. L. Byer and M. Garbuny, "Pollutant detection by absorption using mie scattering and topographic targets as retroreflectors," *Appl. Opt.* **12**(7), 1496–1505 (1973), http://dx.doi.org/10.1364/AO.12.001496.
4. M. J. T. Milton, "Tunable lasers for DIAL applications," *Rev. Laser Eng.* **23**(2), 93–96 (1995), http://dx.doi.org/10.2184/lsj.23.93.
5. N. Menyuk and D. K. Killinger, "Temporal correlation measurements of pulsed dual Co_2 lidar returns," *Opt. Lett.* **6**(6), 301–303 (1981), http://dx.doi.org/10.1364/OL.6.000301.
6. M. J. T. Milton et al., "Injection-seeded optical parametric oscillator for range-resolved DIAL measurements of atmospheric methane," *Opt. Commun.* **142**(1–3), 153–160 (1997), http://dx.doi.org/10.1016/S0030-4018(97)00260-5.
7. S. T. Yang and S. P. Velsko, "Frequency-agile kilohertz repetition-rate optical parametric oscillator based on periodically poled lithium niobate," *Opt. Lett.* **24**(3), 133–135 (1999), http://dx.doi.org/10.1364/OL.24.000133.
8. P. Weibring et al., "Development and testing of a frequency-agile optical parametric oscillator system for differential absorption lidar," *Rev. Sci. Instrum.* **74**(10), 4478–4484 (2003), http://dx.doi.org/10.1063/1.1599065.
9. R. J. Foltynowicz and M. D. Wojcik, "Demonstration of a high output power 1533 nm optical parametric oscillator pumped at 1064 nm," *Proc. SPIE* **7838**(1), 783815 (2010), http://dx.doi.org/10.1117/12.865125
10. "Transmittance of optical materials," Newport.com, p. 444 (2011), http://www.newport.com/Optical-Materials/144943/1033/content.aspx.
11. Savi.weber.edu. Homepage, Hitran database sponsored by Weber State University, http://savi.weber.edu/hi_plot/.